

THE EFFECT OF WHEELS AND WHEELHOUSES ON THE AERODYNAMIC FORCES ACTING ON PASSENGER CARS

Régert Tamás¹, Lajos Tamás²

¹. Assistant Lecturer, ². D.Sc., Professor

*Budapest University of Technology and Economics, Mechanical Faculty,
Department of Fluid Mechanics, Hungary*

ABSTRACT

The aerodynamics of road vehicles has been improved through several decades to almost its optimum, regarding to the shape of the body. However, the unavoidable need for wheels caused and even recently causes significant problems for aerodynamicists to deal with. The addition of wheelhouses and rotating wheels to an aerodynamically optimized car body, leads to an increase in drag- and lift coefficients by 30% and 40%, respectively. Several parameter tests were carried out by means of experiments on models and full scale cars but the attempts to describe the very complex flow were not successful. This article shows the way how wheels change the conditions of the flow around a simplified vehicle model and analyzes the change of forces acting on the different surfaces of the body. General conclusions are drawn from validated CFD results on the mechanism of effect of wheels and wheelhouses on the forces acting on road vehicles.

1. INTRODUCTION

Aerodynamics at cars became more and more important with the increase of their velocity. In the beginning of the 20th century, the shape of vehicles were adopted from the field of aviation and ships. Cars had an aerodynamic shape but their velocity was very low, mainly due to the quality of the roads. A good summary of the historical development of the aerodynamics of road vehicles is summarized in [1].

In the last century, particularly in its last 30 years the possible lowest drag and highest downforce have been approached. The only open question seems to be the reduction of the effect of the rotating wheels facing the flow, or partially covered by the wheelhouse of the car body. The contribution of wheels and wheelhouses to the total aerodynamic drag and lift of a modern car is about 30% and 40%, respectively.

Experiments have already been carried out in recent decades including investigation of full-scale cars [2], model-scale passenger cars [3], and idealized car models [4], [5], [6]. All authors investigating realistic car models concluded that rear wheels have a dramatic effect on the drag, i.e. 2/3 of the above-mentioned 30% contribution to total drag is due to the rear wheels [3]. Elofsson et al. [3] made a parameter study by changing the geometry of the rear spoiler and the fender behind the rear wheel. They found significant changes in drag, emphasizing the importance of the details of interaction between the wake of the wheel and the wake of the body. A parametric study has been made by Fabijanic [4], investigating the effect of the geometry of the wheelhouse on the flow field. In the present work, authors show

the components of the total lift and drag force acting on parts of the vehicle body and their change due to the addition of wheels and wheelhouses. This way the origins of the change of forces can be captured. For the investigation validated CFD model, FLUENT code has been used.

2. METHOD OF INVESTIGATION

For the description of the forces, the flow field has to be determined first. Our choice was made on Computational Fluid Dynamics (CFD) that provides the highest amount of details on the flow field. However, when CFD is used for research purposes, the software has to be validated and verified. The validation and verification process is reported in [7] in detail.

The vehicle model that we used for the investigations, had only one pair of wheels to simplify the problem and can be seen in **Figure 1**.

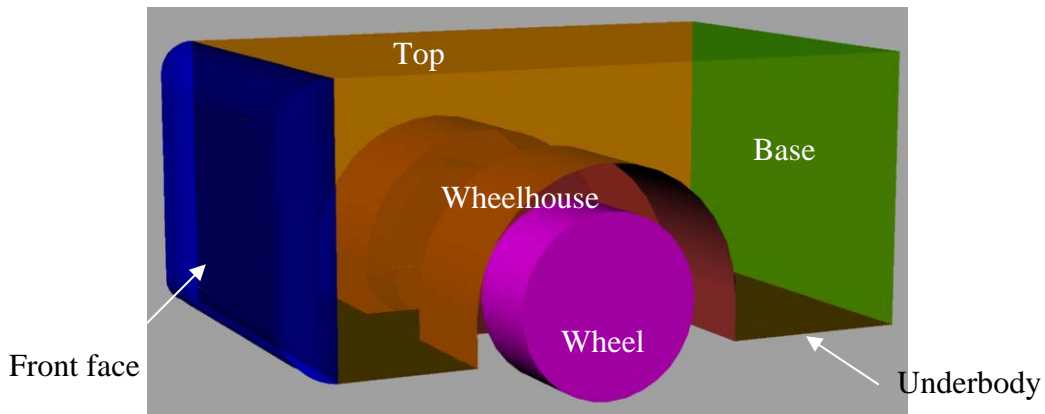


Figure 1. The geometry of the simplified vehicle model of investigation with the indications of the different surfaces

The rounded leading edges of the body provided an approach of the flow without boundary layer separation. The sides are flat, the longitudinal edges are sharp and the wheelhouse has a flat base and cylindrical fender. The wheel is modeled as a solid sharp shouldered cylinder. The height of the body is $0.428L$, the width is $0.643L$. The underbody gap was $1/14L$, or $1/6D$, where $L = 700\text{mm}$ is the length of the vehicle, $D = 300\text{mm}$ is the diameter of the wheel. The rounding radius of the leading edges around the front face of the vehicle model is $R = 50\text{mm}$. The structure of the numerical grid can be seen in **Figure 2**.

The numerical grid consisted of 1,063,000 quad elements and the resolution of the domain was designed according to the concept of RANS (Reynolds Averaged Navier Stokes) equation solving. The Reynolds number based on the diameter of the wheel was $8.5 \cdot 10^5$, i.e. the flow can be considered to be turbulent. The flow was handled to be steady required by turbulence modeling. Reynolds stresses arising from RANS equations were modeled by the concept of turbulent viscosity turbulence models.

As the vehicle model is a bluff body, boundary layer separation occurs and the flow field can be characterized by large volumes of separated flow of low velocities of significant effect. Describing the region of separation bubble is of high

importance when the base pressure is to be determined. However, sharp edges were formed on the vehicle body to fix the location of separation and thus to reduce the uncertainty of this location due to the inaccuracy of the turbulence models.

The 'realizable' $k-\varepsilon$ turbulence [8] model was applied for the computations as it is corrected for stagnation point anomaly [12] and gives a relatively accurate base pressure. Thus forces can be determined within low uncertainty. This turbulence model is also appropriate to compute the size of separation bubbles, though it frequently fails in terms of determination of fine details of the flow inside them [9]. At walls the logarithmic law of the wall was used with modifications to take the effects of pressure gradient into account.

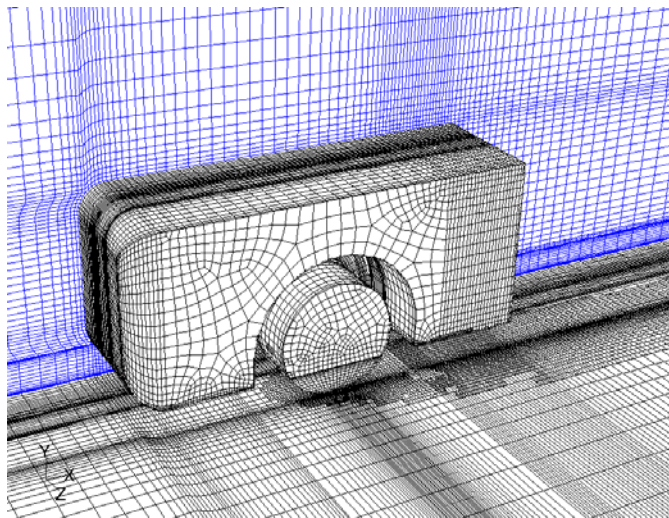


Figure 2. The structure of the numerical grid

Due to the symmetry of the geometry, only one half of the model had to be taken into account. The inlet of the computational domain is at least $5L$ distance in front of the body and the outlet is $10L$ behind the model to avoid significant effect of the boundary conditions on the flow field in the vicinity of the model [10].

At the inlet, a uniform velocity distribution was prescribed. The sides of the domain and also the symmetry plane were Symmetry [13] boundary conditions that set the normal derivative of all variables to zero. The outlet is a pressure outlet that sets the static pressure constant. For discretization, second order upwind schemes were used for the momentum and turbulence equations.

3. RESULTS AND DISCUSSION

3.1 *Flow field around the vehicle*

The aim of the simulations has been to determine the flow field around the vehicle model responsible for the buildup of forces acting on the body. **Figure 3.** shows the streamlines of the steady flow around the vehicle represented in the vertical symmetry plane of the model. Also the filaments of the vortices are visible represented by dots. The boundary layer is forced to separate at the trailing edges of

the base. A large separation bubble forms downstream the base which has a length almost the same as the length of the vehicle itself.

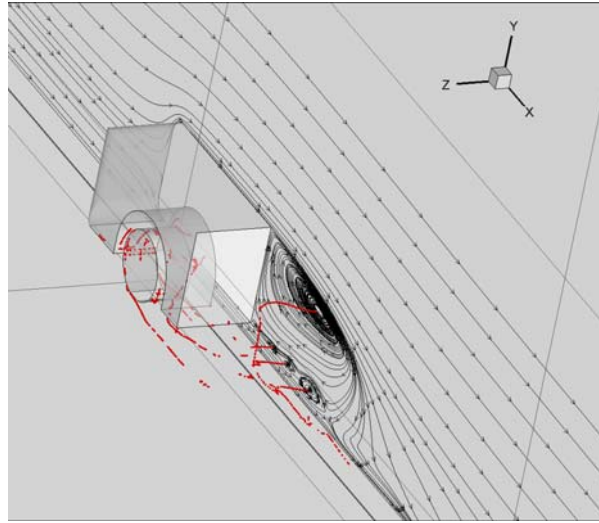


Figure 3. Flow field around the vehicle model. a) Streamlines in the vertical symmetry plane of the vehicle and vortex cores; Flow from left to right.

The cores of the vortices, i.e. the vortex filaments were detected by the method of critical points [11]. These filaments give the possibility of better insight into the structure of the flow field behind the vehicle. The separation bubble contains a large upper vortex, the cross section of which can be seen in **Figure 3**. The lower part of the separation bubble contains smaller vortices. Longitudinal vortices can be observed beside the wheel.

3.2 Forces acting on the vehicle

As the model used at the investigation was symmetrical, we were interested in lift and drag only, the side forces were off the present topic. For mapping the origin of forces and to carry out a systematic study, several geometry configurations were tested. First, a baseline model was created that included wheelhouses and rotating wheels according to **Figure 1**. Then the wheelhouse and the wheel were removed to determine the drag and lift acting on the basic body. The effect of the presence of rotating wheel was investigated by including or removing the wheel from the wheelhouse, and finally, the wheelhouse openings were recursively covered in the presence of rotating wheel. Forces acting on the individual surfaces (shown in **Figure 1**.) are reported here in summary.

Forces are represented in the form of lift and drag coefficients, defined in Eq.(1)

$$C_D = \frac{D}{\frac{\rho}{2} V_\infty^2 A}, \quad C_L = \frac{L}{\frac{\rho}{2} V_\infty^2 A}, \quad (1)$$

where C_D [-] and C_L [-] are the drag and lift coefficients, respectively; D [N] and L [N] are the drag and lift forces, respectively; V_∞^2 [m/s] is the free stream velocity and A [m²] is the streamwise projected total area of the vehicle.

	Drag coefficient		Lift coefficient	
	Basic body	+wheel+wheelhouse	Basic body	+wheel+wheelhouse
front face	0.107	0.147	0.198	0.211
base	0.1476	0.157	0	0
top	0.011	0.0096	0.375	0.4025
underbody	0.00814	0.0073	-0.5387	-0.4319
Partial resultant	0.2737	0.3209	0.0343	0.1816
wheelhouse	-	0.025	-	-0.0905
wheel	-	0.0975	-	0.0998
Resultant	-	0.4434	-	0.1909

Table 1. Drag and lift coefficients on the surfaces of the basic body (no wheels, no wheelhouses) and the baseline model (wheels and wheelhouses are included)

The drag coefficient of the vehicle increases by 62% when wheels and wheelhouses are added to the basic body. Analyzing the components of the drag force one can note that 17% of the increase is originating from the forces acting on the vehicle body due to the modification of the flow field, 9.1% and 35.6% acting on the wheelhouse and the wheel, respectively. One might say that almost 57.4% of the total increase in drag coefficient is the effect of the forces acting on the wheel, while 42.6% of the increase is generated on the body and wheelhouse. However, the wheelhouse contributes in drag only in a very small amount comparing to the wheel.

Lift coefficient changes from 0.0343 to 0.1909 when wheels and wheelhouses were added to the basic body, the lift coefficient of which was, however, very small. The low pressure in the wheelhouse partially cancels the vertical component of forces acting on the wheel and on the wheelhouse and on extending parts of the fender contribute to lift with exerting a downforce on the vehicle. The wheel contributes with 0.0998 and the remaining part of the increase in lift is due to the modification of the flow field and to the pressure increase on the underbody surface of the vehicle in front of the wheels. The wheels block a part of the flow coming in the underbody gap, thus more flow has to move towards the top of the vehicle, generating lower pressure at that region. Thus the pressure on the underbody increases and that on the top of the vehicle decreases, leading to an increase in lift force.

CONCLUSIONS

The flow field around a simplified vehicle model was computed by means of CFD. The geometry, the grid and the computational model is introduced in the paper discussing the details of the flow field around the vehicle model briefly.

The components of aerodynamic forces were determined on different surfaces of the vehicle to show which domains of the flow and how are affected by the addition of wheels and wheelhouses to the basic body. It was concluded that adding wheelhouses and rotating wheels leads to an increase of more than 62% in drag and an even higher increase in lift coefficients. The large change of lift coefficients was due to the small initial lift acting on the basic body.

The force acting on the wheel amounts more than half of the increase in drag and only less than half of that was regarded to the modification of the flow field due to the presence of wheelhouse and rotating wheel. From the drag acting on the wheelhouse and on the wheel separately, one can conclude that the majority of drag increase is generated by the lower part of the wheel which is placed in the underbody gap.

The majority of the increase of lift is, however, due to the modification of the flow field around the body by the wheel. The wheels partially block the flow in the underbody gap that leads a major change in the flow field around the whole vehicle.

REFERENCES

- [1] Hucho W.H.: **Aerodynamics of Road Vehicles**. Butterworth and Co. Publishing, Boston, 1998.
- [2] Wickern, G., Zwicker, K., 1995, "**Zum Einfluß von Rädern und Reifen auf den aerodynamischen Widerstand von Fahrzeugen**", Tagung "Aerodynamik des Kraftfahrzeugs", Haus der Technik e. V., Essen.
- [3] Eloffson, P., Bannister, M., 2002, "**Drag reduction mechanisms due to moving ground and wheel rotation in passenger cars**", SAE paper, 2002-01-0531
- [4] Fabijanic, J., 1996, "**An experimental investigation on wheel-well flows**", SAE paper, 960901
- [5] Skea, A. F., Bullen, P. R., Qiao, J., 1998, "**The use of CFD to predict air flow around a rotating wheel**", 31st. Int. Symposium on Automotive Technology and Automation, Düsseldorf
- [6] Skea, A. F., Bullen, P. R., Qiao, J., 2000, "**CFD simulations and experimental measurements of the flow over a rotating wheel in a wheel arch**", SAE, paper 2000-01-0487
- [7] T. Regert, T. Lajos, 2005, "**Numerical simulation of flow field in wheelhouse of cars**" Journal of Computational and Applied Mechanics, Miskolc
- [8] Shih T. -H., Liou W.W., Shabbir A., Yang Z. and Zhu J.: "**A New k- ϵ Eddy-Viscosity Model for High Reynolds Number Turbulent Flows - Model Development and Validation**", Computers Fluids, 24(3): 227-238, 1995.
- [9] Rodi W.: "**Comparison of LES and RANS calculations of the flow around bluff bodies**", Journal of Wind Engineering and Industrial Aerodynamics 69-71, pp. 55-75, 1997.
- [10] Axelsson, N., Ramnefors, M., Gustafsson, R., 1998, "**Accuracy in computational aerodynamics**", Part I, II., SAE paper, 980037
- [11] Perry A.E., Chong, M.E., Cantwell B.J.: "**A general classification of three-dimensional flow fields**". Phys. Fluids A 2 (5), May 1990. pp. 765-777
- [12] Durbin, P.A., Petterson Reif, B.A.: "**Statistical theory and modelling for turbulent flows**". John Wiley & Sons Ltd. 2001 ISBN: 0 471 49736 3
- [13] Ferziger, J.H., Peric, M.: "**Computational methods for fluid dynamics**". Springer Verlag, Berlin Heidelberg New York, 3rd edition, 2002.